# ASSESSMENT AND IMPROVEMENT OF THERMOELECTRIC PYRANOMETER MEASUREMENTS

Francesco Mariottini[1]*, Giorgio Belluardo[2], Martin Bliss[1], Patrick J. M. Isherwood[1], Ian R. Cole[3], Thomas R. Betts[1]
[1]Centre for Renewable Energy Systems Technology (CREST), Loughborough University
[2]Institute for Renewable Energy - EURAC Research
[3]FOSS Research Centre for Sustainable Energy, University of Cyprus
[1]Loughborough University, LE11 3TU, United Kingdom
[2]Viale Druso 1, 39100 Bolzano (Italy)
[3]University of Cyprus, Nicosia, 2109, Cyprus

ABSTRACT: This work evaluates the variability of thermoelectric pyranometer calibration values seen when using different calibration methods and practices. The pyranometer calibration ISO 9847:1992 standard leaves many procedural details to the user's discretion. The variability resulting from different interpretations influences PV system performance monitoring and energy yield modelling. Improved methods and more robust standardisation are therefore needed to reduce uncertainty in field-deployed thermoelectric pyranometers and consequently reduce risk in PV system energy yield assessment.
This paper investigates the variability induced by relaxed calibration procedures defined in the standard Furthermore, it proposes indoor procedures for the characterisation of pyranometer response to incidence angle and temperature which have not yet been defined in the standards.
Uncertainty of calibration factors including under high angles of incidence and a few cloudy data series from outdoor methods were found to be up to 2.08%, compared with 1.4% stated by the manufacturer. Uncertainty increases up to 4.73% when reference and test sensors are of different types.
Results of indoor calibration procedures agreed to within 1.21% even when calibrating multiple sensors at the same time. The instability of the irradiance source contributed more to the overall uncertainty than the selection of the procedure. The angular response of the devices tested was close to the prescribed limits [1].

Keywords: Calibration, Characterisation, Pyranometer

## 1 INTRODUCTION

Low uncertainties in thermoelectric pyranometer calibrations are often reported based on the stated minimum achievable values for high quality sensors. The reality in the field can deviate considerably from this ideal however, since regular recalibration and attentive maintenance of pyranometers is not always guaranteed. Furthermore, approaches to calibration can also differ significantly and quoted uncertainties may not be commensurate with the device application.

Annex B of ISO 9847:1992 [1] requires the sun to be unobstructed by clouds while performing outdoor calibration for solar energy monitoring applications. The maximum allowed diffuse fraction (diffuse solar irradiance divided by the global solar irradiance) is 0.2 but the time resolution for its calculation is not specified. It also requires that no clouds are within 30° of the sun but the standard allows replacement of this requirement with a non-specified minimum threshold of irradiance to be decided by the user. Annex A [1] lists some type 2c (indoor direct beam apparatus) calibration procedures but the description is not specific enough to repeatedly adapt such procedures to other laboratories having similar, but not identical, equipment. A few previous researchers have investigated changes in outdoor calibration value on angle of incidence [2][3] and compared one indoor and one outdoor methodology [4]. The project for the standard review was registered only in June 2019 and research inputs are also necessary to its development.

The latest version of ISO 9060 [2] published in November 2018 highlights again the importance of reducing pyranometer measurement uncertainty by assessing sensor response to changes in angle of incidence and temperature. Such tests are now required for all types of pyranometer (including thermoelectric pyranometers and reference cells) belonging the highest class (A).

To date there are neither specifications nor agreements on how these tests should be performed. While a few researchers [4] characterised sensor response using a complex setup, alternative solutions are required to meet the demand.

## 2 IMPACT OF DATA HANDLING ON OUTDOOR CALIBRATION VALUES

Effects of different data handling procedures on pyranometer outdoor calibrations have been evaluated using measurements taken by EURAC during clear sky days in June-July 2017 in Bolzano, Italy.

### 2.1 Outdoor calibration: setup

Effects of different data handling procedures were investigated for four pyranometers from two manufacturers against a reference device from the first manufacturer which includes a temperature-compensation system.

The thermoelectric pyranometers were mounted on a thermally isolated structure. All pyranometers were installed in the horizontal plane to within ±1 degree. Data were acquired every ten seconds through a National Instruments cRIO datalogger with the universal module NI-9219 and later averaged over one-minute intervals for analysis.

### 2.2 Outdoor calibration: methodology

Only data corresponding to a maximum solar zenith of 70° degree (calculated through SolPos [5]) were considered. For the outdoor calibration, the following data handling approaches have been compared (Table 1):

**Table 1:** weather data filters and number of measurement series considered for the different approaches: all valid clear sky series (1), one series for representative angle of incidence (2) and no clear sky requirements (3).

| id | beam min [W/m²] | diffuse min [W/m²] | diffuse max [W/m²] | cloud ratio limit | n. of series |
|---|---|---|---|---|---|
| 1 | 700 | 10 | 150 | 0.15 | 32 |
| 2 | 700 | 10 | 150 | 0.15 | 15 |
| 3 | 0 | 0 | 1000 | 1 | 15 |

The mathematical treatment in the standard [1] defines as valid a series whose a minimum number of valid points (21 for the investigated case) show a calibration factor within ±2% of the average calibration factor calculated for all the valid points in the series.
Outdoor calibration uncertainty was calculated by accounting for standard uncertainty from the considered series, data logger uncertainty, reference calibration uncertainty, directional response uncertainty and calibration transfer uncertainty. All uncertainties but the standard uncertainty of the series were based on the datasheet provided by the manufacturer. A coverage factor k of 1.96 was considered.

**Table 2:** overview of considered sources of uncertainty for the abovementioned approaches.

| **subject** | **uncertainty source** | **distribution** | **expanded uncertainty (k=2) [%]** | **Source** |
|---|---|---|---|---|
| reference pyranometer | calibration transfer | normal | 0.5 | manufacturer calibration certificate |
| primary reference | cosine error (in Davos) | normal | 0.5 | manufacturer calibration certificate |
| primary reference | calibration (in Davos) | normal | 1.3 | manufacturer calibration certificate |
| datalogger | gain and offset errors | rectangular | 0.18 | calculated on measured voltage based on manufacturer datasheet |
| measurements | standard deviation | normal | depending on approach | considered valid series |

2.3 Outdoor calibration: results
Without strict requirements on clear sky conditions, uncertainty of the calibration factor increased up to 2.08% due to the impact of datasets corresponding to high angles of incidence and high diffuse fraction conditions. For the pyranometer from the second manufacturer, high deviations were also found for low angles of incidence (and high cloud ratios). Overall uncertainty for the pyranometer increased to 4.73%.

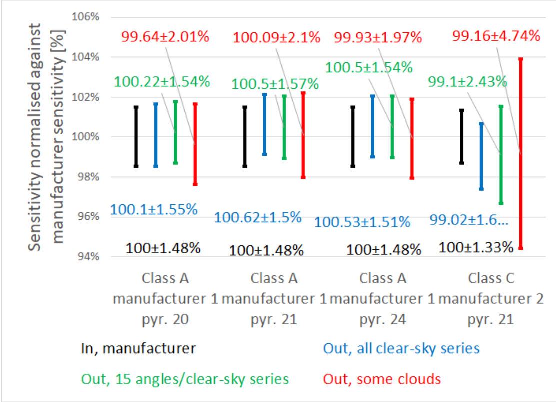


**Figure 1**: Comparison of pyranometer sensitivities calculated through different outdoor calibration approaches.

## 3 COMPARISON OF INDOOR CALIBRATION

Indoor calibration values provided by manufacturer one were compared to calibration values obtained by a single indoor direct beam calibration procedure performing alternate readings based on the MetObs procedure [6] and a newly developed procedure of sequential calibration.

### 3.1 Indoor calibration: setup

The single calibration procedure relies on a class AAA solar simulator using a xenon lamp, a halogen lamp and spectral filters to approximate the AM 1.5G solar spectrum.

The sequential calibrations procedure is based on indoor readings while applying data handling approaches from the outdoor calibration procedure type 1a [6]. Field pyranometers were located in a vertical position inside a ventilated thermal chamber with a glass door facing the artificial light source ARRIMAX 18/12 at a distance of 7.42 m from the sensor plane. Monitored sensor temperatures ranged from 24.27 (first unshaded measurement) to 26.85 °C (last unshaded measurement).

### 3.2 Indoor calibration: methodology

The single indoor calibration under direct beam illumination records five series of measurements, both for the reference and test devices. For each series, dark measurements are recorded first with the light obscured by a shutter. The shutter is then removed and, after 60 seconds, five measurements are taken at intervals of approximately 2 seconds. The overall response is taken as the average of the five series (average light measurements minus average dark measurements) to compensate for any effects of light instability. For the sequential calibrations procedure, unshaded measurements were taken between series of shaded measurements before swapping the position of the reference pyranometer with the next test pyranometer. After a stabilisation phase of 30 seconds, 21 measurements were obtained with an interval of 2 seconds between consecutive measurements.

At the end of the calibration session, a system of equations was used to estimate the calibration factor.
The irradiance measured for each position was calculated through Equation (1) according to the measured voltage $V_{pm}$ referring to a series of M measurements through sensors with calibration factors $f_m$..

$$\bar{\iota}_p = \frac{\sum_{m=1}^{M} f_m \times V_{pm}}{M} \qquad (1)$$

The calibration factor for each sensor was acquired using Equation (2) based on the calibration factor of the reference sensor, $F_R$. For each pair of reference and test sensor, voltages were initially measured when the sensors were at positions p and p+1, respectively.

$$f_s = F_R \times \frac{\left(V_{R(p,m)} + V_{R(p+1,m+1)}\right)}{\left(V_{s(p+1,m)} + V_{s(p,m+1)}\right)} \qquad (2)$$

In the next measurement series, the positions of the sensors were swapped to mitigate any bias due to light source inhomogeneity. The impact of different directional error per pyranometers of the same design and orientation was considered negligible compared to other sources of uncertainty.

### 4.3 Indoor calibration: results

For two pyranometers of manufacturer one, deviations of sequential calibration values from the single calibration values (Jul-Aug 2018) were below 1% on average with a maximum of 1.21% from the manufacturer values. For the third pyranometer of manufacturer one, the newly found calibration value was closer to the manufacturer value (99.92%) compared to the previously calibration value (99.59%).

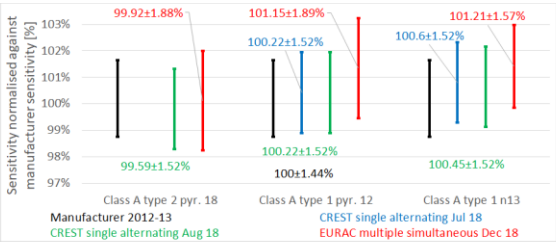


**Figure 2**: Comparison of sensitivities calculated through different indoor approaches.

## 5 CHARACTERISATION PER ANGLE OF INCIDENCE

### 5.1 Characterisation per angle of incidence: setup

The indoor characterisation procedure relies on the previously mentioned ventilated thermal chamber and custom-made manually adjustable platforms. Platforms cover different angles of incidence from 0° to 85°, measured through a Mini Digital Protractor Inclinometer with a 0.1° resolution which, combined with a human error of 0.1°, resulted in a deviation lower than 0.3 as suggested by ASTM G213 [7]. Azimuth orientation of sensors was kept constant corresponding to an orientation of West-North (with North being the cable direction).

The variation in distance from the sensor to the light source were kept to a minimum, with any resulting deviations in irradiance corrected for by application of the measured irradiance uniformity map.

### 5.2 Characterisation per angle of incidence: methodology

The characterisation procedure alternated shaded and unshaded measurements as in the sequential calibration procedure. The ratios of test sensors to reference sensor were first calculated at normal incidence. Then for each unshaded measurement series, the irradiance measured for the reference sensor was multiplied by this ratio and the cosine of the angle of incidence to estimate the theoretical irradiance. Cosine error was calculated as deviation of the measured from the theoretical irradiance [1].

Theoretical irradiance was estimated by accounting for changes of distance from the sensor to the light source. Based on photometric data from the light source manufacturer [8], flux variation with distance was first interpolated through a power function. Then the previously measured irradiance map was scaled for the required distance from the light source.

### 5.3 Characterisation per angle of incidence: results

Response of four pyranometers from the first manufacturer have been investigated for the five angles of incidence requested by the standard [1] and compared to the envisaged values from the standards. Average values were close to the limits for Class A pyranometers equal to limit of ±10(4) $Wm^{-2}$.

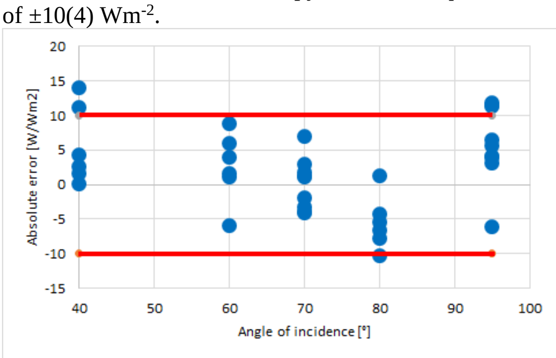


**Figure 3**: Absolute directional errors (corrected to irradiance of 1000 W/m2) measured for four sensors of the same manufacturer and design measured during different sessions.

## 5 CHARACTERISATION PER TEMPERATURE

### 5.1 Characterisation per temperature: setup

Thermoelectric pyranometers were cooled before starting the measurements to compensate the difficulty of cooling the device in the thermal chamber, in particular during the unshaded phase. The temperature of the pyranometers inside the chamber was assumed to be equal to the pyranometer for which the Pt100 temperature sensor was monitored. Temperature of the reference sensor outside the chamber was assumed to be constant for short measurement sessions.

### 5.2 Characterisation per temperature: methodology

The thermal chamber setpoint was varied from 5˚C to 65˚C in steps of 10˚C. For each setpoint value, each unshaded measurement phase was preceded by a shaded measurement phase.

Only the average of the last 21 measurements (timestep of 2 seconds) of each shaded and unshaded phase were considered for further analysis. For each characterisation session, the deviation against the reference response at the temperature closest to 20˚ (20±0.39˚) was calculated. Temperature dependency of the sensitivity was finally obtained by correcting for the irradiance variation measured by the reference sensor $S(T) = \left(\frac{V_{i,meas}(T)}{V_{i,int}(20)} \times \frac{V_{R,int}(20)}{V_{R,meas}(T)}\right) - 1$ (3below (4).

$$S(T) = \left(\frac{V_{i,meas}(T)}{V_{i,int}(20)} \times \frac{V_{R,int}(20)}{V_{R,meas}(T)}\right) - 1 \qquad (3)$$

5.3 Characterisation per temperature: results

For each measurement session, deviations from each session reference were close to the Class A limit of ±1(0,2) %. Results showed a variability among the measurement sessions higher than the variations of temperature reported by the manufacturer (+0.06% and +0.03% respectively for 30˚C and 40˚C).

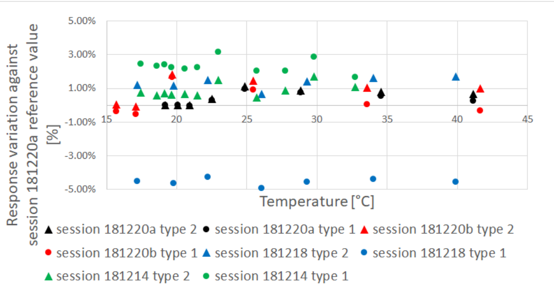


**Figure 4**: Comparison of pyranometer temperature response deviations performed during different sessions.

| Reference temperature | Measures | Average deviations for type 2 pyr. 18 [%] | Average deviations for type 2 pyr. 18 [%] | Average deviations for type 1 pyr. 12[%] | Average deviations for type 2 pyr. 18 [%] |
|---|---|---|---|---|---|
| 20±5 | 18 | 0.02% | 0.57% | 0.00% | 0.61% |
| 30±5 | 11 | 0.25% | 0.53% | -0.04% | 0.56% |
| 40±5 | 3 | 0.19% | 0.57% | -0.35% | 0.79% |

**Table 3:** Temperature response deviations

## 6 CONCLUSIONS

For measurements taken during clear sky days, the uncertainty of calibration factors including high angles of incidence and diffuse fraction were within 2.08% compared to 1.4% stated by the manufacturer. While more relaxed clear sky requirements could be adopted if necessary, it is crucial to use reference sensors of the same type to avoid an excessive increase in uncertainty (up to 4.73% within this work).

Results of indoor calibration procedures agreed to within 1.21% even when calibrating multiple sensors at the same time. The instability of the irradiance source was the main contributing factor to the overall uncertainty. Still, uncertainty of the calibration factors could be reduced by using more stable light sources or efficiently increasing the number of measurements in each time period.

The determined values of sensor angular response were higher than the expected prescribed limits for Class A pyranometers in some cases. Further research is required to deal with unwanted uncertainties due to irradiance distribution and angle of incidence (i.e. lack of uniformity and collimation error)

Gradual variations of temperature, as well as an accurate monitoring of the irradiance and temperature in the reference and test sensors seem to be crucial in reducing the uncertainty in temperature response characterisation.

The findings suggest how calibration methods could be adapted to different conditions while maintaining an acceptable degree of confidence in the results.

Uniform light source and accurate temperature monitoring are crucial for characterisation of thermoelectric pyranometer response respectively to angle of incidence and temperature. That would ultimately reduce uncertainty in field-deployed pyranometers and consequently reduced risk in PV system energy yield assessment.

## 7 ACKNOWLEDGEMENTS


This study has received funding from the European Union's Horizon 2020 research and innovation programme under the Marie Sklodowska-Curie grant agreement No 721452.

The authors would like to thank David Cennamo, Valentino Diener and Fabio Bertoletti for their help with the practical setup of the calibration and characterisation procedures at EURAC.


## 8 REFERENCES


[1] ISO, "ISO 9060:2018 Solar energy - Specification and classification of instruments for measuring hemispherical solar and direct solar radiation," vol. 2018. 2018.

[2] A. Habte, M. Sengupta, A. Andreas, I. Reda, and J. Robinson, "Radiometer calibration methods and resulting irradiance differences," *Prog. Photovoltaics Res. Appl.*, vol. 25, no. 7, pp. 614–622, 2017.

[3] A. Driesse, W. Zaaiman, D. Riley, N. Taylor, and J. S. Stein, "Investigation of Reference Cell and Photodiode Calibrations under Different Conditions," *Ieee Pvsc*, pp. 1–5, 2016.

[4] A. Driesse, W. Zaaiman, D. Riley, N. Taylor, and J. S. Stein, "Indoor and Outdoor Evaluation of Global Irradiance Sensors," no. September, pp. 14–18, 2015.

[5] NREL, "Solar Position and Intensity." .

[6] BSI, "BS 7621-1993 ISO 9847:1992 Method for calibrating field pyranometers by comparison to a reference pyranometer." 1993.

[7] ASTM, "G213 − 17 Standard Guide for Evaluating Uncertainty in Calibration and Field Measurements of Broadband Irradiance with Pyranometers," no. May, pp. 1–16, 2017.

[8] ARRI AG, "Arrimax 18/12," 2019. [Online]. Available: https://www.arri.com/en/lighting/daylight/m-series/arrimax-18-12. [Accessed: 24-Jul-2019].